JOURNAL OF THERMOPHYSICS AND HEAT TRANSFER
Vol. 7, No. 2, April–June 1993

Thermal Contact Conductance of a Phase-Mixed Coating Layer by Transitional Buffering Interface

K. C. Chung,* J. W. Sheffield,† H. J. Sauer Jr.,‡ and T. J. O'Keefe§
University of Missouri-Rolla, Rolla, Missouri 65401
and
A. Williams¶
Monash University, Melbourne, Australia

The thermal contact conductances of metallic joints having phase-mixed coating layers applied by a novel transitional buffering interface technique was investigated. This study is restricted to relatively low contact pressure and to microhardness (P/H) ratios, $10^{-4} < P/H < 6 \times 10^{-4}$, where very little data exist. These results are extremely useful for some applications such as electrical contacts in spacecraft. The purposes of this work were 1) to conduct an experimental study to examine four different coating materials, two pure materials, and two phase-mixed materials; and 2) to develop a theoretical model for a phase-mixed coating layer to predict the thermal contact conductance under the first-load cycle. The theoretical model included both the thermal and mechanical (microhardness) aspects of the contact problem. An extensive experimental program was carried out employing four different coating materials, as well as a broad range of surface roughness and microhardness. In order to obtain more robust coatings than conventional methods with better endurance, an adhesion test was conducted to investigate the adhesive strength of transitional buffering interface (TBI) coating layers.

Nomenclature

A = area of cylindrical rod for adhesion test, m^2
A_a = apparent area of contact, m^2
A_r = real area of contact, m^2
a = contact spot radius, m
D = Vickers indentation depth, m
F_a = force required to pull out the coating layer, N
H = microhardness, Pa
H_p = predictive microhardness from experimental correlations, Pa
H' = effective microhardness, Pa
h = thermal contact conductance, W/m^{2}K
h' = thermal contact conductance for coating layer, W/m^{2}K
k' = effective thermal conductivity, W/mK
L = static load, N
l = surface asperity slope
N = number of contact spots
P = contact pressure, Pa
R = thermal contact resistance, K/W
t = coating layer thickness, m
ε = dimensionless radii ratio of a contact spot to heat flux tube
σ = surface roughness
Ψ = dimensionless thermal constriction parameter

Subscripts
1 = region 1
2 = region 2

Superscript
′ = layer

Presented as Paper 91-1396 at the AIAA 26th Thermophysics Conference, Honolulu, HI, June 24–26, 1991; received Oct. 10, 1991; revision received April 5, 1992; accepted for publication May 11, 1992.

*Research Assistant, Department of Mechanical and Aerospace Engineering and Engineering Mechanics.
†Professor of Mechanical and Aerospace Engineering. Senior Member AIAA.
‡Professor of Mechanical and Aerospace Engineering.
§Curators' Professor of Metallurgical Engineering.
¶Associate Professor of Mechanical Engineering.

Introduction

DURING the last decade, a considerable amount of research and study has been devoted to the problem of predicting thermal contact resistance/conductance of metallic contacts. Publications not only emphasize the importance of this research topic, but also indicate that the development of a predictive model has proven to be a difficult task. Most research works focus on the bare metallic theoretical/experimental contact analysis. Only a few consider surface treatments such as surface preparation, as well as the addition of chemically deposited or vapor deposited materials on the surfaces. This aspect makes it more difficult to develop a theoretical model to predict the thermal contact conductance at the interface because the phase-mixed coating layer may considerably change both the mechanical and thermal characteristics at the interface compared with those of the underlying metal. The phase-mixed coating is believed to be novel and the analysis herein is confined to contact between similar, nonwavy, flat, and isotropically rough surfaces in a vacuum environment.

The literature focusing on the use of metallic coatings to enhance thermal contact conductance is somewhat limited. In 1965 Fried and Kelley[1] presented results of their experiments using stainless steel samples with vapor-deposited magnesium and aluminum coatings for contact pressure ranging from 0 to 8 MPa. They concluded that the use of vapor-deposited metallic coatings could improve the contact conductance for harder base metals. However, no general correlation or model was presented. O'Callaghan et al.[2] presented the first work concerning the thermal contact of coated surfaces where the experimental data are accompanied by the detailed surface texture of the test specimens. Unfortunately, the experimental setup was limited in heat flow capacity that caused low interface temperature differences and cast doubt on the reliability of the test results. Kang et al.[3] evaluated the effect on the thermal contact conductance of turned surfaces using three different coating materials (lead, tin and indium) and the results verified that an optimum coating thickness existed. They also indicated that the thermal contact conductance en-

hancement was greater at lower contact pressure. However, they did not examine the effect of surface roughness on the enhancement of the thermal contact conductance. In 1990, Ochterbeck et al.[4] conducted an experiment to examine new materials which can enhance the thermal contact conductance while simultaneously being electrically insulating. Only one insulating material, Isostrate, a polyimide film coated with a paraffin-based compound, provided an increase in the thermal contact conductance. Because there are many materials for coating and no standard method for measuring or reporting the topography of the contacting surface, a suitably general correlation for a coated metal junction has not been achieved. Antonetti[5] developed a thermal-mechanical model for a nominally flat, conforming rough surface as follows:

$$(h'\sigma/lk') = 1.25(P/H')^{0.95} \quad (1)$$

This model was developed for ranking combinations of layer-substrates in terms of the effective thermal conductivities and effective hardnesses of the substrate and coating material. The model compared quite well with limited experimental results obtained for smooth silver coatings on one contacting side of a pair of bead-blasted nickel specimens. A dimensionless correlation for anodized aluminum coatings that related the overall joint conductance to the coating thickness, the surface roughness, and the contact pressure was developed by Peterson and Fletcher[6] as follows:

$$(h't/k')(t/\sigma)^{0.25} = 0.83 \times 10^{-2}(P/H') + 0.11 \times 10^{-4} \quad (2)$$

Seven specimens, varying in coating thickness from 60.9 to 163.8 μm, were tested and the contact pressure ranged from 0 to 14 MPa.

Basically, one- and two-surface coatings can employ the same theoretical analysis. It is well known[7] that the asperities of most practical engineering surfaces have rounded summits and the peak angle is characteristically in the range of 160–170 deg. This means that when two such high points touch, the contact resembles that made by two hemispheres. Thus, it is reasonable to model the contact as a circular spot. Then, each microcontact can mathematically be associated with a circular heat flux cylinder.

In one of the more recent investigations, Antonetti[5] developed a predictive model which can apply to a two-surface coating. However, no verified experimental work was undertaken for two-surface coating specimens. Nevertheless, this model could serve as an excellent starting point for the development of a predictive model of two-surface phase-mixed coatings. In another study, Sheffield et al.[8] attemped to find a practical way to reduce the thermal contact resistance for an aircraft electronic box. The specimen pairs consisted of bare, single, and double-sided coatings of aluminum, indium, and lead. A total of 33 specimens pairs were tested in vacuum under numerous loading pressures. The report by Sheffield is the most recent work concerning the thermal contact of two-surface coated specimens where the data are accompanied by detailed surface characteristics and coating thicknesses of the test samples. Their report presents the results of an investigation of thermal contact conductance involving 1) the effects of surface roughness on thermal contact conductance for a low contact pressure, and 2) an experimental investigation of two-surface coatings compared with the experimental results of one-surface coatings. However, they did not provide a comparison between a model and the tested data.

The use of transitional buffering interface (TBI) metallic coatings to enhance thermal contact conductance has been studied experimentally by Chung et al.[9,10] To study the effect of coating thickness and materials, steady-state conductive heat transfer experiments were conducted. The improvement of the thermal contact conductance for pure copper coatings was greater than copper-carbon phase-mixed coatings by 10–20% depending upon the contact pressure and contact surface characteristics. However, a theoretical model was needed to compare with the experimental data.

Theoretical Model

When two conforming rough surfaces are brought into contact under a static load, intimate contact occurs only at a discrete number of microcontact spots whose total area is a small fraction of the apparent contact area. Under vacuum conditions with negligible radiation, heat transfer across the interface only takes place by conduction through microcontacts.

We can assume that the micro-contact spot radius is very small compared with the distance separating it from the neighboring contacts, and therefore, the constriction resistance is obtained from the classical solution by Holm[11] for a single circular disc of radius a on a half-space with thermal conductivity k:

$$R = (1/4ka) \quad (3)$$

As the microcontacts grow in size and increase in number, a function $\Psi(\varepsilon)$ must be introduced to allow for the interference between the heat flux tubes. Now the thermal constriction resistance for a semiheat flux tube can be written as

$$R = [\Psi(\varepsilon)/4ka] \quad (4)$$

where $\Psi(\varepsilon)$ is the thermal constriction parameter.

The thermal constriction resistance for the ith heat flux tube is

$$R_i = \frac{\Psi_{i1}(\varepsilon)}{4k_1a} + \frac{\Psi_{i2}(\varepsilon)}{4k_2a} \quad (5)$$

It is assumed that there are N isothermal flat microcontacts randomly distributed over the apparent area, and each microcontact has a circular geometry of radius a. Taking these microcontacts to be in parallel with each other yields

$$\frac{1}{R} = \sum_{i=1}^{N}\left[\frac{\Psi_{i1}(\varepsilon)}{4k_1a} + \frac{\Psi_{i2}(\varepsilon)}{4k_2a}\right]^{-1} \quad (6)$$

Since the specific thermal contact conductance is defined by

$$h = (1/RA_a) \quad (7)$$

Substituting Eq. (6) into Eq. (7) yields

$$h = \frac{N}{A_a}\left[\frac{\Psi_1(\varepsilon)}{4k_1a} + \frac{\Psi_2(\varepsilon)}{4k_2a}\right]^{-1} \quad (8)$$

It is well-established that flow pressure is related to the pressure under a blunt indenter in a static hardness indentation test. However, it has been shown by Tabor[12] that the Vickers hardness value is almost equal to the flow pressure for isotropic solid contacts. Therefore, at the contact surface the ratio of the real to the apparent area is

$$(A_r/A_a) = (P/H) \quad (9)$$

Because the real area is equal to the area of a mean microcontact of radius a multiplied by the number of microcontacts N, Eq. (9) can be rewritten as

$$N = (A_a/\pi a^2)(P/H) \quad (10)$$

By substituting Eq. (10) into Eq. (8), the general expression for the thermal contact conductance across an interface of dissimilar materials in a vacuum becomes

$$h = \frac{4}{\pi a}\frac{P}{H}\left[\frac{\Psi_1(\varepsilon)}{k_1} + \frac{\Psi_2(\varepsilon)}{k_2}\right]^{-1} \quad (11)$$

In Eq. (11), the mean microcontact spot radius a is given by Yovanovich[13]

$$a = 0.99(\sigma/l)\{-\ell n[3.132(P/H)\}^{-0.547} \quad (12)$$

Antonetti and Yovanovich[14] had shown that the expression for the thermal contact conductance across a joint with a layer on both sides of the contact can be obtained by rewriting Eq. (11) as

$$h' = \frac{4}{\pi a'}\frac{P}{H'}\left[\frac{\Psi_1'(\varepsilon)}{k_1} + \frac{\Psi_2'(\varepsilon)}{k_2}\right]^{-1} \quad (13)$$

Because of geometric symmetry about the contact plane, we can put

$$\Psi_1'(\varepsilon) = \Psi_2'(\varepsilon) = \Psi'(\varepsilon) \quad (14)$$

Introducing Eq. (14) into Eq. (13) and using the harmonic mean thermal conductivity, we obtain

$$h' = \frac{2}{\pi a'}\frac{P}{H'}\frac{k'}{\Psi'(\varepsilon)} \quad (15)$$

In Eq. (15), two important paramets, k' and a', are

$$k' = \frac{2k_1k_2}{k_1 + k_2} \quad (16)$$

$$a' = 0.99(\sigma/l)\{[-\ell n[3.132(P/H')]\}^{-0.547} \quad (17)$$

Microhardness Analysis

Hegazy[15] investigated the variation of hardness with depth of indentation and determined the relation between the Vickers microhardness and the indentation size. The most common technique for measuring microhardness is the static indentation test. A static indentation test has the advantage of providing a very simple nondestructive means for assessing the resistance of material to plastic deformation. In a static indentation test, a steady load is applied to an indenter and the hardness is calculated from the area or depth of indentation produced.

Mulhearn[16] showed that the hardness values for different shape indenters are in good agreement under same load for the same material. Hence, one can determine the contact hardness for a set of microhardness on the basis of equal indentation areas. In other words, the contact hardness value can be estimated from Vickers microhardness variation as a function of the asperity spot radius. This yields the following relationship between a Vickers half-diagonal (a_v) and an asperity spot radius (a):

$$a_v = \sqrt{(\pi/2)}\, a \quad (18)$$

Next, employing l, the Vickers indentation depth can be written as

$$D = l\sqrt{(\pi/2)}\, a \quad (19)$$

In the static indentation test, an indenter is pressed into the surface and the hardness value (MPa) is expressed as the ratio of the load to the area of the impression

$$H = (1.8544L/D^2) \quad (20)$$

where L is the static load (N) and D is the indentation depth (mm).

It is assumed that the relation between the static load and the resulting indentation depth is given by

$$L = cD^n \quad (21)$$

where c and n are constants. Then, by combining Eqs. (20) and (21), the following relationship can be obtained for microhardness:

$$H = 1.8544cD^{n-2} \quad (22)$$

or, we can express it as

$$H = c_1D^{c_2} \quad (23)$$

where c_1 and c_2 are constants.

An approximate expression for the mean contact spot radius is[13]

$$a = 0.99(\sigma/l)\{-\ell n[3.132(P/H)]\}^{-0.547} \quad (24)$$

substituting Eqs. (19) and (24) into Eq. (23), we obtain a general expression of the microhardness as

$$H = c_1(1.24\sigma)^{c_2}\{-\ell n[3.132(P/H)]\} - 0.547c_2 \quad (25)$$

Because the indentation depth depends upon the microhardness, and the depth must be known to determine the microhardness, an iterative approach is required to obtain the accurate microhardness values.

Experimental Program

An experimental investigation is being conducted to determine the thermal contact conductance at the interface of contacting aluminum 6061-T651 surfaces using a new process of surface coating—TBI. The manufacturing process involves plasma-enhanced deposition onto a surface of either conducting (metallic) or insulating (nonmetallic) base material. The plasma-deposited thin coating is typically a two-phase mixture of copper and carbon or silver and carbon. The relative ratio of carbon to copper or carbon to silver can be varied by altering the deposition parameters, giving the desired chemical concentration gradient through the coatings. The process appears to offer excellent characteristics of adhesion of coating to a wide range of base materials, and very close control of coating thickness and of surface roughness.

Thermal Experimental Apparatus and Specimens

The experimental facilities used in this investigation, along with the details of the facility construction and operating conditions, have been reported by Chung.[17] An experimental apparatus has been modified to measure the thermal contact conductance of a large set of coated and uncoated pairs of metal specimens. The apparatus consisted of a heating and cooling system, a pneumatic pressure cylinder, a load bellows, a bell jar, and pairs of test specimens. The experimental apparatus used in this investigation is shown in Fig. 1. Each specimen has designated primary and secondary contacting surfaces. Each pair, with their primary surfaces facing together, were placed in a vertical alignment with the two heat flowmeters forming a vertical stack. Each heat flowmeter, which is made of 304 stainless steel, is approximately 10.16-cm (4-in.) long and 2.54-cm in diameter.

Each heat flowmeter contained four thermocouples along the longitudinal axis of the cylinder. The thermocouple holes, which are 1.59-mm (0.0625-in.) in diameter, were drilled perpendicular to the axes of the flowmeters. Thermocouples, made of 28 gauge copper-constantan, were placed in the holes making physical contact with the centerline of the specimen. Upon installation of those thermocouples, a thermal grease was used to fill these holes. The thermocouple leads were wrapped around the test cylinders to minimize conduction error. The heat source was an electrical heater with a regulated power supply. The temperature of the test interface was kept constant with the use of a temperature controller to regulate the heater. Prior to testing, the labeled specimens were stored in a desiccant container in order to minimize

effects of oxidation. A two-stage mechanical vacuum pump was used to maintain the required vacuum pressure level of approximately 0.2 Torr in the bell jar in order to reduce the convection effects in the test facility.

All test specimens were fabricated from a single aluminum 6061-T651 rod. Contact surfaces were prepared on the faces of 2.54-cm diam by 2.54-cm long cylindrical specimens. The end of the specimens were carefully turned to produce smooth and flat surfaces. The surface roughness of all the test specimens were controlled between 0.23–0.32 μm.

The specimens were, of course, tested later in pairs. Each pair was treated further by four different surface treatments, polished, turned, blasted-smooth and blasted-rough, at both of its primary surfaces to a predetermined roughness. Blasted-smooth and blasted-rough surfaces were produced by a jet of air with entrained glass beads. After this process, the specimens were cleaned using acetone and distilled water. The contacting surface characteristics of each test specimen was measured with a Perthometer model C5D made by Feinprueft Corporation. Profilometer measurements of the flat surfaces indicated the average roughness ranged from 0.15 to 6.0 μm. Pertinent test specimen characteristics are shown in Table 1.

A stainless steel 304 of known thermal conductivity used as a standard reference heat flowmeter resulted in a correlation for the thermal conductivity (W/mK) of the aluminum 6061-T651 of

$$k = 13.36 + 0.382T(K) \tag{26}$$

Thermal conductivity was determined over 55–63°C temperature range. The data was curve-fitted using a linear regression analysis to obtain the value of thermal conductivity. The averaged experimental uncertainty in the measurement of the thermal conductivity of aluminum 6061-T651 was estimated at 9.9% corresponding to the thermocouple reading system.

Each specimen, or test sample, was coated on one surface with a very thin layer of metal, which was applied by the TBI technique. Four different coating materials, pure copper, pure silver, two phase mixture copper-carbon and silver-carbon, were used to produce the coating on aluminum 6061-T651 substrate. TBI is a new process of surface coating being developed in the Graduate Center for Material Research of the University of Missouri-Rolla.[18,19] The pure coatings or graded phase-mixed coatings were layered onto aluminum substrate by glow discharge plasma. A capacitively coupled bell jar-type reactor as shown in Fig. 2, operating at a frequency of 10 kHz, was used for plasma creation. Either a single or double diode magnetron electrode system was used to create a plasma. Two copper/silver plates (18 × 18 cm) were used as the electrodes for a single electrode system, and two titanium plates were added as the second set of electrodes for a double electrode system. A sample mounting disk was located in the middle of the diode and rotated at 50 rpm for uniform plasma coatings. Composition graded coating were layered by simultaneous sputter deposition of electrode material with plasma polymerization using a methane (CH_4) monomer and argon carrier. A discharge power of 80 W was supplied to the titanium plates for 5 min to try to obtain a high degree of chemical bonding between the plasma coating and substrate. Next, the supply power (60 W) was switched to the copper electrode plate to incorporate the copper into the coating by sputter deposition; then, changing the discharge power every 2 min from 80 to 140 W in 20 W incre-

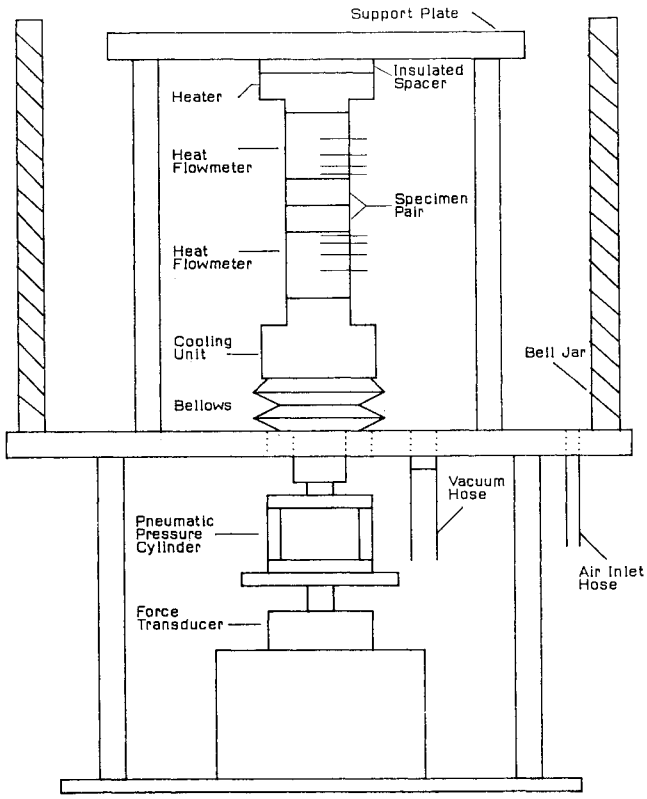

Fig. 1 Schematic of experimental apparatus.

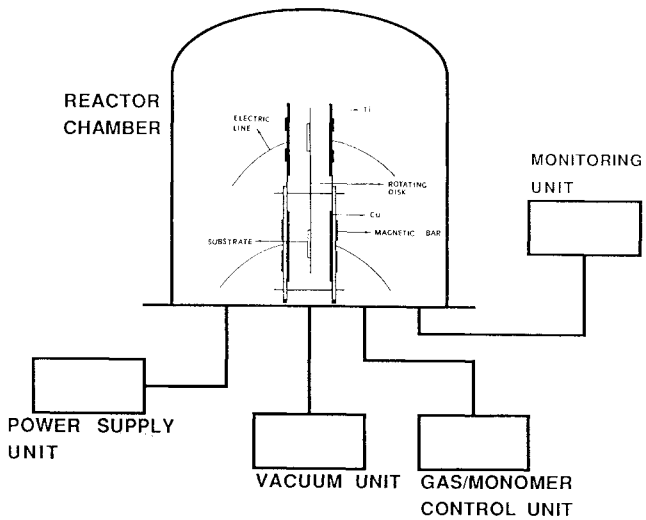

Fig. 2 Plasma reactor system.

Table 1 Test specimens characteristics

No.	Specimens	Coating materials	Coating thickness, μm	Surface roughness, μm	Asperity slope, rads
1	101/102	Cu/C	0.25	0.15/0.17	0.025/0.019
2	103/104	Cu/C	0.45	0.26/0.29	0.046/0.048
3	105/106	Cu/C	0.45	1.91/1.66	0.270/0.200
4	107/108	Cu/C	0.25	2.62/2.85	0.378/0.395
5	109/110	bare	none	0.45/0.39	0.013/0.012
6	111/112	bare	none	1.32/1.32	0.031/0.032
7	113/114	bare	none	3.20/3.20	0.179/0.141
8	115/116	bare	none	5.50/5.70	0.202/0.196
9	117/118	Cu	0.19	0.17/0.23	0.028/0.025
10	119/120	Cu	0.19	0.29/0.32	0.051/0.046
11	135/136	Cu	0.24	2.27/2.29	0.274/0.276
12	137/138	Cu	0.24	2.96/2.74	0.306/0.295
13	121/122	Ag	0.23	0.18/0.17	0.022/0.026
14	123/124	Ag	0.23	0.32/0.32	0.054/0.069
15	145/146	Ag	0.24	2.16/2.31	0.233/0.258
16	129/130	Ag	0.24	3.06/3.14	0.323/0.350
17	131/132	Ag/C	0.18	0.23/0.20	0.032/0.031
18	133/134	Ag/C	0.18	0.26/0.23	0.033/0.030
19	147/148	Ag/C	0.39	1.98/2.11	0.287/0.291
20	143/144	Ag/C	0.39	2.13/2.41	0.395/0.435

ments and keeping the discharge power at 140 W till the coating thickness achieved the value desired. The composition of the graded coating layers which changes from 100% carbon to nearly pure copper/silver metallic over the thickness of the coating layer, eliminates sudden changes in physical and chemical structures between two dissimilar materials and assists in establishing a stronger, more durable interface.

An uncertainty analysis was performed to estimate the maximum uncertainty associated with the measured contact conductance under vacuum environment. The probable experimental uncertainty is estimated to be less than 8%.

Microhardness Test

In order to use the value of microhardness for the prediction of thermal contact conductance, four different coating materials (pure copper, pure silver, copper-carbon, and silver-carbon) were tested. The tested surfaces were prepared on the faces of 2.54-cm long, 2.54-cm diam cylinder. In order to reflect microhardness values accurately, all the polished specimens were chosen. Five different samples used to make microhardness measurements are 1) uncoated aluminum, 2) TBI pure copper coatings, 3) TBI copper-carbon coatings, 4) TBI pure silver coatings, and 5) TBI silver-carbon coatings. Most frequently, loads which were employed in Vickers microhardness measurements, lie in the range 500–10 g. The typical loads used in the present work were 500, 300, 200, 100, 50, 25, and 10 g. All the test process were conducted at a constant indoor temperature of 70°F. A least-square fit of the Vickers microhardness measurements for the previously mentioned materials, using Eq. (22), gives the following correlations:

Bare Specimens

$$H_p = 1.46D^{-0.102} \tag{27}$$

Pure Cu

$$H_p = 1.36D^{-0.08} \tag{28}$$

Cu/C

$$H_p = 1.365D^{-0.086} \tag{29}$$

Pure Ag

$$H_p = 1.35D^{-0.082} \tag{30}$$

Ag/C

$$H_p = 1.406D^{-0.0896} \tag{31}$$

where D is the Vickers indentation depth.

The above correlations show that the microhardness value is inversely proportional to the power of the indentation depth so that the microhardness increases with decreasing indentation depth. It is clear that as the indentation depth increases, the microhardness value gradually approaches substrate (aluminum 6061-T651) values. In summary, the predicted value of the microhardness from the correlations match the measurements with maximum percent difference of 3.5. Therefore, based upon the good agreement between the microhardness measurements and the predictions for those materials, Eqs. (27–31) can be used for predicted thermal contact conductance as a satisfactory description of microhardness variation in relation to different TBI coating materials.

Results and Discussion

Almost 150 experimental data points have been obtained from one series of bare aluminum 6061-T651 specimens and four series of different coatings specimens made from TBI coating technique. These series consist of 20 thermal tests, each series consists of 4 different surface roughnesses thermal tests, polished surfaces, turned surfaces, blasted-smooth surfaces, and blasted-rough surfaces, each of about two days duration. These tests covered a broad range of contact pressures, surface textures, and surface microhardness variations.

The first series of tests was performed using four pairs of bare aluminum 6061-T651 specimens having a broad range of surface parameters. Thermal tests of uncoated specimens were undertaken for considering the zero-layer thickness case which can be the basis data and compared with available general correlations in the open literature to show their similarities and differences. In order to compare the test results graphically with the present contact conductance model, the normalizing contact pressure has been used. One empirical correlation for predicting thermal contact conductance under light contact load were developed by Hegazy.[15] He correlated his experimental data as a function of dimensionless parameter C_c, and proposed the following correlation:

$$C_c = (h\sigma/lk) = 0.22(P/H)^{0.714} \tag{32}$$

The comparison will be made possible by plotting the dimensionless contact conductance, $(h\alpha/lk)$ against the contact pressure for nominal values of surface parameters, contact microhardness and contact pressures. The graphical comparison between the experimental and dimensionless contact conductance values, as a function of the relative contact pressure, are presented in Fig. 3 and the pressure was normaized with respect to the contact hardness of each pair. As can be seen from the figure the agreement between the experimental and the correlation developed by Hegazy is good for blasted surface specimens and the root mean square (rms) percent difference for these series is 17.4%. However, the overall rms percent difference for all the uncoated specimens is 22.4%. One of the potential reasons for the variation between the experimental data and Eq. (32) may be the contact surface is flat, but not totally optical flat.

Comparison Between Theory and Test Results

Table 2 presents the parameters involved in the calculation of the theoretical contact conductance for a typical phase-

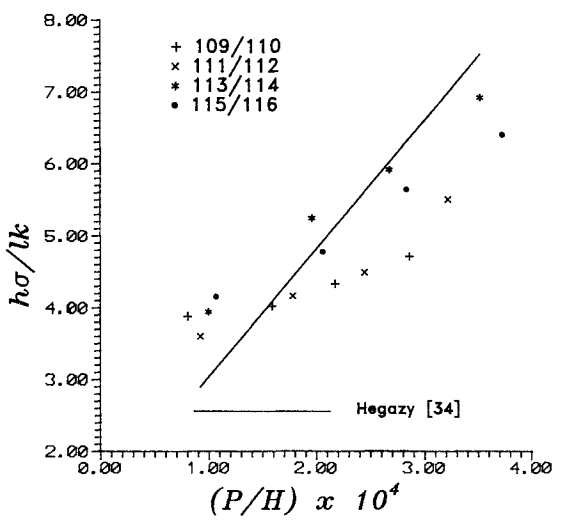

Fig. 3 Dimensionless contact conductance for uncoated specimens.

Table 2 Calculated theoretical parameters relating to contact conductance for a typical phase-mixed specimen pair. Specimen no. 101/102, σ = 0.227 and l = 0.032

Run	P, kPa	H', GPa	$k'/\Psi'(\varepsilon)$, W/mK	a', μm	h', kW/m^{2}K
1	134.8	1.681	39.20	2.21	0.91
2	268.7	1.674	37.38	2.32	1.66
3	372.5	1.670	36.49	2.37	2.19
4	482.8	1.668	35.77	2.42	2.73

mixed coatings specimen pair and illustrates the steps in predicting the contact conductance. P is measured from pressure gauge and combined with H', which came from the experimental correlations, and a' were obtained from Eq. (17). Finally, when the thermal constriction parameter[20] $\Phi'(\varepsilon)$ is known, the thermal contact conductance can be found by evaluating Eq. (15).

The experimental data presented in this investigation indicate the difficulty of characterizing thermal contact conductance of phase-mixed coating layers. A suggested approach to this problem involves defining the phase-mixed contacts in term of the established contact theory. Thus, the predicted values of thermal contact conductance of phase-mixed coatings, generated with Eq. (15), are compared to corresponding experimental data. The relationships expressed in Eq. (15) involve parameters found important in influencing phase-mixed contact heat transfer. Along with contact pressure, these include surface roughness, surface asperity slope, microhardness, and thermal conductivity of the contact surface. The comparisons between the experiments and predictions are presented in Figs. 4 and 5. Figure 4 shows the measured and predicted thermal contact conductance plotted against the contact pressure for phase-mixed copper-carbon coatings pairs. As expected, the thermal contact conductance increases with an increase in contact pressure. Clearly, it can be seen that the agreement between the experiment and theory is not good at the first point for each set. The measured conductance is considerably higher than the prediction for these first points,

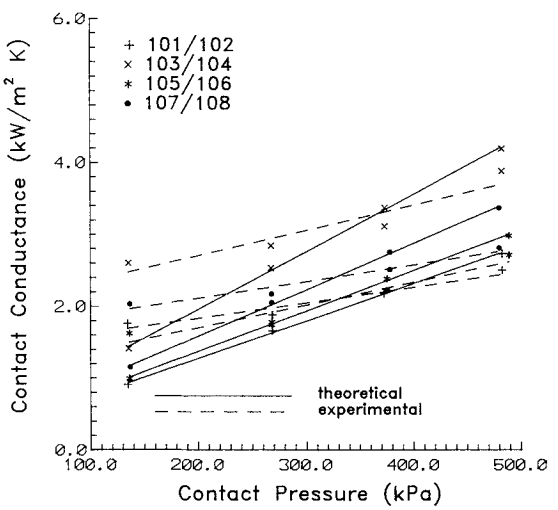

Fig. 4 Comparison between theory and test results for Cu/C specimens.

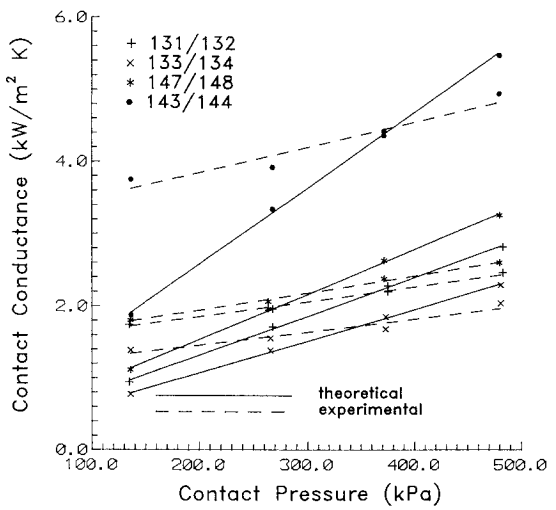

Fig. 5 Comparison between theory and test results for Ag/C specimens.

but tends towards the theoretical line at next points. The rms percent difference for the next three points for each test set is 10.6%. However, the overall rms percent difference for all 16 test points is 25.3%. The slopes of the experimental data line are lower than that of theoretical predictions. The same behavior can be observed for different surface textures. Figure 5 demonstrates a comparison between the measured conductance and the predicted values for the silver-carbon coatings pairs. It can be seen that the characteristics of the experimental data are quite similar to the copper-carbon test pairs. The deviation between the first data points and the theory is also significantly higher, although this deviation decreases rapidly with increasing applied load. The overall RMA percent difference between the experiment and theory for silver-carbon coatings specimens is 26.6%, while the rms percent difference for the rest of the 12 data points is only 13.7%. One possible explanation for discrepancies between experimental and predicted results is believed to occur because of the difficulty in controlling the exact gradient of carbon within the phase-mixed coatings. The very low thermal conductivity of carbon would be expected to be influential on the thermal contact conductance of phase-mixed coatings. However, the deviation between the experiments and the predictions also depends upon the surface roughness, contact pressure, and thermal flux.

Adhesion Test Results

The adhesion of coatings is an important parameter in both optical and electronic applications. Also, a diagnostic tool can indicate durability and environmental stability when developing thin coatings processes. Under repeated compressive contacts, some conventional coatings have shown imperfect adhesion which renders such surfaces unacceptable for use in specific purposes such as the thermal control system design of high speed aircraft. For potential applications, such as protective coatings, some military specifications apply for scratch resistance, temperature cycling, specified loading cycling, etc., and quantitative information is desired about the adhesive strengths.[21] The most common mechanical methods for measuring adhesion are peeling method, scratch method, and direct pull method.

Peeling method ("tape test") is an extremely simple method to perform the adhesive tests. In its simplest version, a piece of adhesive tape is pressed against the coating layer. The test consists of observing whether the coating is peeled off or not when the tape is removed. Sometimes, the peeling method did not work, since strongly adherent coatings cannot be stripped off the substrate at all.

In the scratch method, a fine but smooth stylus is drawn across the coating layer. The load on the stylus, which is required to cause peeling, is taken as a measure of coating layer adhesion. However, the behavior of the metal coatings under test is very complex resulting in difficulties in the interpretation of the results.

In contrast to these two methods, the direct pull method is geometrically simple and should, in principle, lend itself to an interpretation in terms of forces of adhesion per unit area. A pin or cylinder is bonded to the coating layer by cement. The normally applied force which is required to remove the coating layer is then measured. Detail of the direct pull method was described by Bhasin et al.[22] as shown in Fig. 6. The force F is applied at the rods and directed through the center of the substrate. The pulling force is transferred to two cylindrical blocks which are cemented to the substrate. Assuming that the force required to pull the coating layer off the substrate is F_f, the force of adhesion F_a per unit area is defined by

$$F_a = (F_r/A) \tag{33}$$

where A is the area of the cylindrical rod. The TBI coating layer at different surface roughnesses on aluminum substrate were measured for their adhesion.

In order to establish the thermal characteristics of coatings, it is important to examine the mechanical adhesion property of TBI coatings. Some experiments on conventional coatings/films subjected to repeated normal compressive contacts have shown imperfect adhesion in several cases, which renders such surfaces unacceptable for their intended uses in the thermal control systems.

In order to compare all adhesive strength with different coating materials and different finished surface types, 12 samples were tested and the results are summarized in Table 3. First examined were the copper and copper-carbon samples. The turned surface have similar values for samples nos. 119 and 103. But the blasted-smooth surface copper-carbon sample showed higher adhesive strength than that of pure copper sample. Second, the silver-carbon coating specimens produced higher adhesive strength than pure silver coating specimens. Basically, the rough surface samples produced higher adhesive strength than smooth surface samples. It is interesting to note that the silver-carbon smooth surface samples, nos. 132 and 134, can obtain higher strength than that of rough surface sample, no. 144. From Table 3, we found that the silver-carbon samples, nos. 132 and 134, are 2.05 and 2.43 times larger adhesive strength than pure silver samples, nos. 121 and 123, respectively. Nevertheless, the adhesive strength of blasted-smooth specimen no. 144 is only 45% higher than specimen no. 145. It is believed that the smooth surface might obtain more significant adhesion effect than rough surface for adopting phase-mixed coating layers.

In conclusion, the phase-mixed coating layer exhibited stronger adhesion than pure coatings layers. The coating thicknesses seem to have no influence on adhesive strength. However, different coating materials and a wide range surface roughnesses are needed to be examined in order to substantiate this preliminary result.

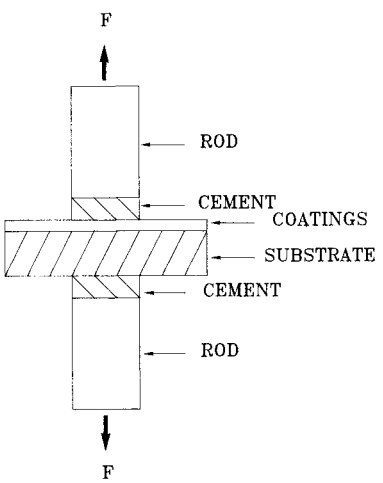

Fig. 6 Adhesion test setup.

Table 3 Adhesive strength of TBI coatings

Specimens no.	Finished type	Coating material	Coating thickness, μm	Adhesive strength, kPa
119	T	Cu	0.19	7,723
136	B/S	Cu	0.24	7,585
138	B/R	Cu	0.24	10,129
103	T	Cu/C	0.45	7,343
106	B/S	Cu/C	0.45	9,550
121	P	Ag	0.23	4,930
123	T	Ag	0.23	4,847
145	B/S	Ag	0.24	8,688
123	B/R	Ag	0.23	8,922
132	P	Ag/C	0.18	15,024
134	T	Ag/C	0.18	16,638
144	B/S	Ag/C	0.39	12,639

P, polished surface; T, turned surface; B/S, blasted-smooth surface; and B/R, blasted-rough surface.

Conclusions

The TBI coating method is one of the most promising techniques in thin coating technology because it can produce pinhole-free, fine-grained coatings with unique chemical and physical properties. These unique properties are normally due to the variation of coatings composition which is controlled by the operating conditions of the glow discharge deposition. In this investigation, both primary surfaces of each pair of specimens were coated with a pure Cu and Ag or a phase mixture of Cu/C and Ag/C.

Different specimen surfaces exhibit different microhardness variations which depend primarily upon the material type and secondarily upon the machining process. For the tested materials, a semiempirical microhardness variation model has been proposed as a function of indentation depth. Therefore, microhardness variations can be presented with acceptable accuracy for both of pure Cu and Ag and phase-mixed Cu/C and Ag/C coatings using simple power law expressions.

The good agreement between the measured and predicted contact conductance verifies the validity of the phase-mixed coatings model over a broad range of surface roughness, and contact pressure for materials possessing a wide range thermophysical properties. However, there still existed some discrepancies between experimental and theoretical results. The deviations between the contact conductance data and predicted results are partly a result of the gradient of carbon within the phase-mixed coatings. Minor damage to these prepared surfaces could have an exaggerated effect on their thermal contact behaviors.

In addition to establishing the thermal characteristics of TBI coatings, the mechanical integrity and adhesion properties were also examined. A direct pull method was applied to measure the adhesive strength between the coatings and substrates. The experimental results provide an important indicated parameter for coating durability and stability. Based on these results, the silver-carbon coating specimens can produce stronger adhesive strength than pure silver coating specimens by a factor 1.45–2.43. The limited test data for Cu and Cu/C coating specimens indicated that the copper-carbon sample (no. 106) offered 20% higher adhesive strength than pure copper coatings sample (no. 136).

References

[1]Fried, E., and Kelley, M. J., "Thermal Conductance of Metallic Contacts in a Vacuum," *Thermophysics and Temperature Control of Spacecraft and Entry Vehicles*, edited by G. B. Heller, Vol. 18, Progress in Aeronautics and Astronautics, AIAA, New York, 1966, pp. 697–718.

[2]O'Callaghan, P. W., Snaith, B., Probert, S. D., and Al-Astrabadi, F. R., "Prediction of Interfacial Filler Thickness for Minimum Thermal Contact Resistance, *AIAA Journal*, Vol. 21, No. 9, 1983, pp. 1325–1330.

[3]Kang, T. K., Peterson, G. P., and Fletcher, L. S., "Effect of Metallic Coatings on the Thermal Contact Conductance of Turned Surface," ASME National Heat Transfer Conf., ASME Paper 89-HT-23, Philadelphia, PA, Aug. 6–9, 1989.

[4]Ochterbeck, J. M., Fletcher, L. S., and Peterson, G. P., "Evaluation of Thermal Enhancement Films for Electronic Packages," *Proceedings of the 9th International Heat Transfer Conference*, Israel, 1990, pp. 445–450.

[5]Antonetti, V. M., "On the Use of Metallic Coatings to Enhance Thermal Contact Conductance," Ph.D. Dissertation, Univ. Of Waterloo, Waterloo, Ontario, Canada, 1983.

[6]Peterson, G. P., and Fletcher, L. S., "Measurement of the Thermal Contact Conductance and Thermal Conductivity of Anodized Aluminum Coatings," *Journal of Heat Transfer*, Vol. 112, No. 3, 1990, pp. 579–585.

[7]Kubo, M., "Statistical Analysis of Surface Roughness Waveforms," *Annals of C.I.R.P.*, Vol. XIV, 1967, pp. 279–288.

[8]Sheffield, J. W., Sauer, H. J., Jr., and Look, D. C., Jr., "Thermal Contact Resistance Studies of Ion Deposition Processed Samples,"

Final Rept., McDonnell Douglas Corp. PO-Z50050, Vols. 1 and 2, Feb. 1986.

[9]Chung, K. C., Sheffield, J. W., Sauer, H. J., Jr., O'Keefe, T. J., and Williams, A., "An Experimental Study of Enhancing Thermal Contact Conductance by Transitional Buffering Interface (TBI)," AIAA 29th Aerospace Sciences Meeting, AIAA Paper 91-0490, Reno, Nevada, 1991.

[10]Chung, K. C., Sheffield, J. W., Sauer, H. J., Jr., O'Keefe, T. J., Zhang, J., and Williams, A., "Effects of Transitional Buffering Interface Coatings on Thermal Contact Conductance," AIAA 26th Thermophysics Conf., AIAA Paper 91-1396, Honolulu, HI, 1991.

[11]Holm, R., *Electrical Contacts Handbook*, 3rd ed., Springer-Verlag, Berlin, 1958.

[12]Tabor, D., *The Hardness of Metals*, Oxford University Press, Oxford, England, UK, 1952.

[13]Yovanovich, M. M., "Thermal Contact Correlations," *Spacecraft Radiative Transfer and Temperature Control*, edited by Thomas E. Horton, Vol. 83, Progress in Astronautics and Aeronautics, AIAA, New York, 1982, pp. 83–95.

[14]Antonetti, V. W., and Yovanovich, M. M., "Enhancement of Thermal Contact Conductance by Metallic Coatings: Theory and Experiment," *Journal of Heat Transfer*, Vol. 107, 1985, pp. 513–519.

[15]Hegazy, A. A., "Thermal Joint Conductance of Conforming Rough Surfaces: Effects of Surface Microhardness Variations," Ph.D. Dissertation, Univ. of Waterloo, Waterloo, Ontario, Canada, 1985.

[16]Mulhearn, T. O., "The Deformation of Metals by Vickers-Type Pyramidal Indenters," *Journal of Mechanics and Physics of Solids*, Vol. 7, 1959, pp. 85–96.

[17]Chung, K. C., "Thermal Contact Conductance of a Phase-Mixed Coating Layer by Transitional Buffering Interface," Ph.D. Dissertation, Mechanical Engineering, Univ. of Missouri-Rolla, Rolla, MO, 1992.

[18]Sun, B. K., "Metallization of Nonconducting Substrates by Means of Transitional Buffering and Micro-Dendritic Films," Ph.D. Dissertation, Metallurgical Engineering, Univ. of Missouri-Rolla, Rolla, MO, 1989.

[19]Iriyama, Y., "Plasma Polymerization and Plasma Treatment for Modification of Surfaces of Polymeric Materials," Ph.D. Dissertation, Chemistry Dept., Univ. of Missouri-Rolla, Rolla, MO, 1989.

[20]Chung, K. C., Sheffield, J. W., and Sauer, H. J., Jr., "Thermal Constriction Resistance of Phase-Mixed Metallic Coatings," *Fundamental of Conduction*, ASME HTD-Vol. 173, Minneapolis, MN, July 28–31, 1991, pp. 27–33.

[21]Jacobsson, R., "Measurement of the Adhesion of Thin Films," *Thin Solid Films*, Vol. 34, 1976, pp. 191–199.

[22]Bhasin, K., Jones, D. B., Sinharoy, S., and James, W. J., "The Adhesion of Thin Plasma-Polymerized Organic Films to Metal Substrates," *Thin Solid Films*, Vol. 45, 1977, pp. 195–202.